RSC Sustainability

ROYAL SOCIETY OF CHEMISTRY

PAPER

View Article Online
View Journal | View Issue

Cite this: *RSC Sustainability*, 2026, **4**, 1857

Sustainable itaconamide monomers from amino acids for vat photopolymerization 3D printing

Rosario Carmenini, †[a] Filippo Capancioni, †[a] Mirko Maturi, [b] Erica Locatelli, [a] Sergio I. Molina, [b] Letizia Sambri [a] and Mauro Comes Franchini *[a]

Vat photopolymerization (VP) is a rapidly growing additive manufacturing technology (3D-printing), yet its reliance on fossil-derived and potentially hazardous acrylate resins presents a significant sustainability challenge. Although itaconic acid has emerged as a promising bio-based platform chemical, current synthetic strategies to functionalize it often involve toxic intermediates and energy-intensive processes. This work reports a sustainable route for the synthesis of a novel class of itaconamide monomers derived from essential amino acids (alanine, valine, isoleucine, and phenylalanine) *via* the direct, solvent-minimised ring-opening of itaconic anhydride. This approach avoids chlorinated reagents and activation steps, aligning with green chemistry principles. The monomers were incorporated into photocurable formulations (up to 40 mol%), demonstrating highly tunable mechanical properties: aliphatic derivatives acted as efficient plasticizers, increasing elongation at break by up to 385%, while phenylalanine moieties provided network reinforcement *via* π–π interactions. Thermal analysis confirmed stable glass transition temperatures combined with enhanced char yields. Crucially, a quantitative sustainability assessment yielded a Sustainable Formulation Score (SFS) of up to 51.8, significantly outperforming current state of the art bio-based resins. The successful fabrication of high-resolution 3D printed objects confirms these materials as viable, high-performance, and eco-friendly candidates for VP.

Received 8th January 2026
Accepted 13th February 2026

DOI: 10.1039/d6su00014b

rsc.li/rscsus

Sustainability spotlight

SDG number 9 and 13. This research directly supports UN Sustainable Development Goal 9 (Industry, Innovation and Infrastructure) by enabling more sustainable advanced manufacturing technologies, and Goal 13 (Climate Action) by promoting material solutions that reduce reliance on fossil-derived, resource-intensive resin systems. This work advances sustainable materials development for additive manufacturing by introducing itaconamide monomers derived from amino acids through a simplified, low-impact synthetic route. By avoiding hazardous activating agents and reducing synthetic complexity, the study demonstrates how photocurable resins for vat photopolymerization can be redesigned to lower environmental burden while retaining high-resolution 3D printing performance. The resulting materials exhibit tunable mechanical properties and are quantitatively assessed using a holistic sustainability metric, moving beyond conventional bio-based content indicators.

Introduction

As declared in the last ASTM International's Wohlers Report, the Additive Manufacturing (3D-printing) market has grown by 9.1% in 2024, confirming the positive trend that has existed for ten years, reaching USD 21.9 billion of value.[1] In this field, vat photopolymerization (VP) represents one of the most used process, enabling the creation of a series of high-resolution objects with micron-size detailing using UV-cured liquid resins. VP offers unmatched resolution and design freedom, but the sustainability of photopolymer resins remains a significant challenge because the acrylate and methacrylate-based systems that are mainly derived from fossil resources may release hazardous substances during use and disposal,[2,3] therefore studies on VP have highlighted the urgent need for sustainable resin formulations. The sustainability of these resins depends on several factors, such as the feedstock origin, the synthetic route, the printing and post-curing energy demand, and the end-of-life options.[4,5] About the feedstock origin, several bio-based resins have already been explored using these processes: vegetable oils and fatty acid derivatives can be epoxidized or acrylated to yield flexible UV-curable monomers.[6,7] Carbohydrate-based precursors such as isosorbide, sorbitol, and vanillin provide rigid, hydroxyl-rich frameworks for tuneable networks.[8,9] Lignin-derived phenolics introduce aromatic rigidity and have been recently demonstrated as effective components in photopolymerizable systems for VP.[10,11] Thiol-based monomers have been successfully integrated into vat photopolymerization resins, leveraging radical thiol-ene polymerization to enable rapid curing, reduced shrinkage

[a]*Department of Industrial Chemistry "Toso Montanari", University of Bologna, Bologna 40136, Italy. E-mail: mauro.comesfranchini@unibo.it*

[b]*Dpto. Ciencia de los Materiales, I. M. y Q. I., IMEYMAT, Facultad de Ciencias, Universidad de Cádiz, Campus Río San Pedro, s/n, 11510 Puerto Real, Cádiz, Spain*

† Authors contributed equally.

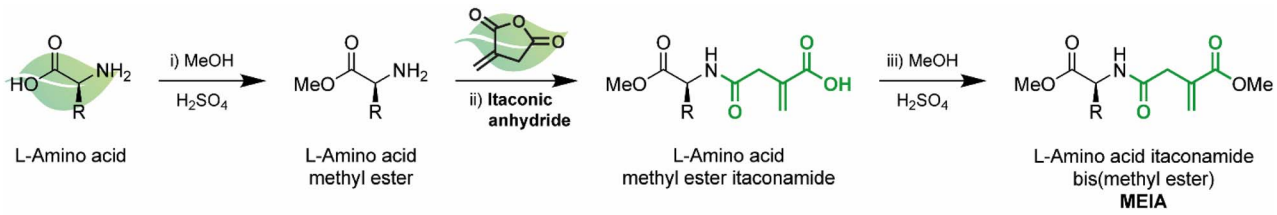

Fig. 1 Synthetic pathway for the synthesis of itaconamide, which include (i) Fischer esterification of the amino acid esterification in methanol, with sulfuric acid as the catalyst, (ii) synthesis of itaconamide intermediates (IA), and (iii) a second Fischer esterification to achieve MEIA derivatives. Steps (ii) and (iii) were analogously performed on *n*-octylamine to compare AA-derived products with the analogous produced using a primary aliphatic amine.

stress, and tuneable network degradability.[12] Together, these example classes demonstrate how the natural pool can decrease dependence on fossil-derived acrylates and support the development of more sustainable VP resins. Within this context, itaconic acid (IA) is particularly promising. Produced fermentatively from renewable biomass, IA is recognized as a platform chemical for sustainable polymers.[13] Its derivatives have enabled recyclable polyurethane networks and photopolymerizable polyesters, highlighting its potential in resin development for VP.[14] The library of renewable feedstocks for vat photopolymerization (VP) can be significantly expanded beyond the currently explored bio-acrylates.[15,16]

Amino acids are particularly attractive due to their abundance, structural diversity, and tuneable reactivity, while short peptides offer modular combinations that can impart biodegradability and bio-functionality to photopolymer networks.[5,17] In parallel, platform chemicals like itaconic acid,[18] remain versatile intermediates for novel resin architectures.[15,19] However, most synthetic routes reported to obtain itaconate-based acrylates, polyesters, or urethanes rely on activated intermediates such as itaconoyl chloride, epoxides, or acid halides, which require hazardous reagents and energy-intensive conditions.[19,20] For example, bio-based VP resins derived from itaconic acid often employ chlorination with thionyl or oxalyl chloride to form reactive esters or amides.[21,22] These approaches, while effective, produce stoichiometric halogenated by-products and involve multiple purification steps, resulting in high E-factors (defined as the ratio between the mass of waste generated and the mass of the desired product)[23] and increased process energy demand. Conversely, the direct ring-opening of itaconic anhydride with bio-based nucleophiles (amines, alcohols, or thiols) provides a more straightforward and sustainable route to functional monomers suitable for photopolymerization. This reaction proceeds under mild, solvent-minimized conditions without the need for chlorinated reagents or activation steps, offering improved atom economy and reduced waste generation. Such a direct approach aligns with green chemistry principles and represents a viable low-impact alternative for producing itaconamide or itaconate-based resins compatible with VP. Furthermore, itaconic anhydride is a readily available intermediate derived from bio-fermentative itaconic acid, simplifying the overall synthetic pathway and reducing its environmental footprint. Within this broader context, the design of itaconamide-based monomers from amino acids stands out as a promising and complementary route toward sustainable VP resins.

In this work, we report the synthesis of a new series of Methyl Ester ItaconAmide monomers (MEIA) derived from essential amino acids, obtained through the direct ring-opening of itaconic anhydride, thereby avoiding the use of reactive intermediates such as itaconoyl chlorides or epoxides (Fig. 1). All reactions have been conducted according to the principles of green chemistry, aiming to minimize the environmental footprint by using green solvents and low-energy purification procedures. To study and optimize the reaction parameters and the regiochemical outcome of the nucleophilic attack, a simple aliphatic primary amine was initially employed as a model substrate. Phenylalanine was selected to introduce an aromatic moiety, while alanine, valine, and isoleucine provided aliphatic side chains with different lengths and branching, offering a diversified set of substituents to investigate structure–property relationships. These monomers were incorporated into a VP photocurable resin at up to 40 mol%, keeping the mono/bifunctional co-monomer ratio constant, yielding sixteen formulations. The resins were mechanically and thermally tested and used to print high-resolution objects, confirming that these monomers preserve the dimensional accuracy typical of vat photopolymerization while supporting a more sustainable synthetic route for resin development.

Materials and methods

All chemicals were purchased from Sigma-Aldrich (St. Louis, MO, USA) and used as received. A series of itaconamide (bis) methyl ester derivatives were synthesized following a unified three-step procedure involving: (i) esterification of the amino acid (when required), (ii) formation of the itaconamide intermediate (IA), and (iii) final methyl esterification to afford the corresponding MEIA derivative.

For all reactions, commercially available reagents were used without further purification. All solvents were dried when necessary, and reactions were conducted under a nitrogen atmosphere. Detailed differences between the synthesis procedure of the different MEIA derivatives are reported in Table S1.

Esterification of the amino acid

The selected amino acid (0.12 mol) was dispersed in methanol (200 mL) in a 1 L round-bottom flask equipped with a magnetic

stirrer and a reflux condenser. Concentrated sulfuric acid (9.6 mL, 0.18 mol) was added, and the suspension was heated to reflux under nitrogen for the required reaction time (24–72 h depending on the amino acid). After cooling to room temperature, the solvent was removed under reduced pressure to afford the corresponding methyl ester hydrogensulphate, which was used in the following step without additional purification.

Me-Ala: yield ≥ 98%. ^{1}H-NMR (600 MHz; DMSO-d_6): 8.24 (s, 2H); 4.02 (m, 1H); 3.73 (s, 3H); 1.39 (s, 3H). Me-Phe: yield ≥ 98%. ^{1}H-NMR (600 MHz, DMSO-d_6): 8.39 (s, 3H); 7.20–7.35 (m, 5H); 4.30 (q, 1H); 3.66 (s, 3H); 3.12 (dd, 1H); 3.05 (dd, 1H).

Me-Ile: yield ≥ 98%. ^{1}H-NMR: (600 MHz, DMSO-d_6): 8.27 (d, 3H); 3.95 (m, 1H); 3.73 (s, 3H); 1.86 (m, 1H); 1.43 (m, 1H); 1.24 (m, 1H); 0.87 (dt, 6H).

Me-Val: yield ≥ 98%. ^{1}H-NMR: (600 MHz, DMSO-d_6): 8.28 (s, 3H); 3.93 (m, 1H); 3.76 (s, 3H); 2.12 (m, 1H); 0.96 (d, 3H); 0.94 (d, 3H).

Synthesis of the itaconamide intermediate

The amine or amino acid methyl ester hydrosulfate (0.12 mol) was suspended in an appropriate organic solvent (300 mL of ethyl acetate or 2-MeTHF, depending on the synthesis) and neutralized with either Na_2CO_3 (25.4 g, 0.24 mol) or $NaHCO_3$ (40.3 g, 0.48 mol). The mixture was cooled to 0 °C, and itaconic anhydride (13.5 g, 0.12 mol), dissolved in 100 mL of solvent, was added dropwise. After completion of the addition, the reaction mixture was allowed to warm to room temperature and was stirred for 24 h (or 2 h in the case of *n*-octylamine). The resulting suspension was filtered, and the solvent was removed under vacuum to yield the corresponding itaconamide intermediate (IA) as a solid or viscous liquid, typically in quantitative yield.

Oct-IA: yield 53%. ^{1}H-NMR (600 MHz, $CDCl_3$): 6.41 (s, 1H); 6.04 (s, 1H); 5.88 (s, 1H); 3.23 (m, 4H); 1.49 (m, 2H); 1.27 (m, 10H); 0.87 (t, 3H). ESI-MS [M+Na$^+$]: 264.

Ala-IA: yield ≥ 98%. ^{1}H-NMR (600 MHz, DMSO-d_6): 11.11 (s, 1H); 9.37 (s, 1H); 5.70 (s, 1H); 5.15 (s, 1H); 4.21 (m, 1H); 3.59 (s, 3H); 2.98 (dd, 2H);1.24 (s, 3H). ESI-MS [M−1]: 214.

Phe-IA: yield ≥ 98%. ^{1}H-NMR (600 MHz, DMSO-d_6): 8.37 (d, 1H); 7.19–7.30 (m, 5H); 6.05 (s, 1H); 5.54 (s, 1H); 4.44 (m, 1H); 3.58 (s, 3H); 3.09 (m, 2H); 3.00 (m, 1H); 2.89 (m, 1H). ESI-MS: [M+Na$^+$]: 314.

Ile-IA: yield ≥ 98%. ^{1}H NMR (600 MHz, DMSO-d_6): 8.20 (d, 1H);6.09 (s, 1H); 5.64 (s, 1H); 4.23–4.19 (m, 1H); 3.62 (s, 3H); 3.22–3.12 (dd, 2H) 1.42–1.37 (m, 1H); 1.23–1.14 (m, 1H); 0.85–0.82 (m, 6H). ESI-MS: [M−1]: 256.

Val-IA: yield ≥ 98%. ^{1}H NMR (600 MHz, DMSO-d_6): 8.27 (d, 1H); 6.06 (s, 1H); 5.60 (s, 1H); 4.14 (m, 1H); 3.62 (s, 3H); 3.22–3.12 (dd, 2H) 3.17 (m, 1H); 2.01 (m, 1H); 0.85–0.82 (m, 6H). ESI-MS: [M−1]: 242.

Final esterification to afford MEIA derivatives

The itaconamide intermediate (0.12 mol) was dissolved in methanol (200 mL) in a 1 L round-bottom flask equipped with a magnetic stirrer. Sulfuric acid (9.6 mL, 0.18 mol) was added, and the mixture was heated to reflux under nitrogen for 2 h. After cooling to room temperature, methanol was removed under reduced pressure. The crude residue was dissolved in 2-MeTHF, neutralized with solid $NaHCO_3$, filtered, and dried over sodium sulfate. The solvent was removed under vacuum, and the residue was washed with diethyl ether to afford the corresponding MEIA derivative, typically in quantitative yield.

Oct-MEIA: yield ≥ 98%. ^{1}H-NMR (600 MHz, $CDCl_3$): 6.41 (s, 1H); 6.32 (s, 1H); 5.94 (s, 1H); 3.77 (s, 3H); 3.22–3.19 (m, 4H); 1.46 (m, 2H); 1.27 (m, 10H); 0.87 (t, 3H). ESI-MS [M+Na$^+$]: 278.

Ala-MEIA: yield ≥ 98%. ^{1}H-NMR (600 MHz, DMSO-d_6): 11.11 8.37 (d, 1H); 6.14 (s, 1H); 5.70 (s, 1H); 5.74 (s, 1H); 4.25 (m, 1H); 3.59 (s, 3H); 3.66 (s, 3H); 3.61 (s, 1H); 3.17 (s, 2H); 1.24–1.27 (d, 3H). ESI-MS [M+Na$^+$]: 252.

Phe-MEIA: yield ≥ 98%. ^{1}H-NMR (600 MHz, DMSO-d_6): 8.41 (d, 1H); 7.30–7.20 (m, 5H); 6.10 (s, 1H); 5.62 (s, 1H); 4.46 (m, 1H); 3.60 (s, 3H); 3.58 (s, 3H); 3.13 (m, 2H); 3.03–2.88 (m, 2H). ESI-MS: [M+Na$^+$]: 328.

Ile-MEIA: yield ≥ 98%. ^{1}H NMR (600 MHz, DMSO-d_6): 8.24 (d, 1H); 6.13 (s, 1H); 5.71 (s, 1H); 4.21 (m, 1H); 3.64 (s, 3H); 3.62 (s, 3H); 3.27–3.19 (dd, 2H); 1.80–1.73 (m, 1H); 1.42–1.37 (m, 1H); 1.22–1.15 (m, 1H); 0.86–0.81 (m, 6H). ESI-MS: [M−1]: 272.

Val-MEIA: yield ≥ 98%. ^{1}H NMR (600 MHz, DMSO-d_6): 8.27 (d, 1H); 6.06 (s, 1H); 5.60 (s, 1H); 4.14 (m, 1H); 3.64 (s, 3H); 3.62 (s, 3H); 3.22–3.12 (dd, 2H) 3.17 (m, 1H); 2.01 (m, 1H); 0.85–0.82 (m, 6H). ESI-MS: [M+Na$^+$]: 280.

Formulation of photocurable resins

Photocurable formulations were prepared by dissolving each MEIA derivative in a mixture of isobornyl methacrylate (IBOMA), 2-phenoxyethyl acrylate (EGPEA) and 1,6-hexanediol diacrylate (HDDA) with the addition of 2 g of ethyl (2,4,6-trimethyl benzoyl) phenyl phosphinate (Et-APO) and 1 g of 2,6-ditert-butyl-4-methylphenol (BHT) per 100 g of base resin in a fixed-speed planetary mixer (Precifluid P-MIX100) for 4 minutes. Each formulation, reported in details in Table S2, has been selected so that the following conditions were satisfied in all cases: (i) the weight ratio of IBOMA to EGPEA was 1 : 1 in all cases; (ii) the concentration of acrylate groups coming from the crosslinking HDDA was equal to 16.8 mol% in all formulations; (iii) the concentration of photocurable groups coming from the MEIA derivatives was equal to either 10, 25 or 40 mol%.

VP 3D printing of photocurable resins

Specimens for tensile test have been designed using computer-assisted design (CAD) following the ISO-37 Type 2 specifications (5 × 2 mm^2 cross-section, 25 mm gauge length). The 3D models were sliced using Chitubox Pro V 2.0 software. First, the .stl files corresponding to the tensile test specimens were imported onto the virtual plate, and then the printing parameters (such as layer height, exposure time, and lifting speed) were configured before slicing into the corresponding g-code. The layer height for all specimens was 0.05 mm, and the irradiation time per layer was optimized for each formulation, ranging from 50 to 120 seconds. The g-code files were exported, and all specimens were printed using a Phrozen Sonic 8K 3D printer equipped with a 7.1-inch 50 W monochrome 405 nm LCD-LED screen with an *XY* resolution of 22 μm. Tensile dogbone specimens were

printed directly onto the build plate, without the use of supports, with their longitudinal axis lying parallel to the *XY* plane. After printing, the samples were detached from the build plate, washed with isopropanol to remove uncured resin, and post-cured for 120 min at 60 °C in a UV curing oven (FormCure, Formlabs) equipped with a 405 nm light source (1.25 mW cm^{-2}).

Chemical and mechanical characterization

^{1}H and ^{13}C NMR spectra were obtained on Varian Inova (14.09 T, 600 MHz) and Varian Mercury (9.39 T, 400 MHz) NMR spectrometers. Regioselectivity of itaconic anhydride aminolysis was assessed by comparing the integrals of the signals corresponding to the methylene group of itaconic acid, which are different for each regioisomer. Mass spectra were recorded on a micro mass LCT spectrometer using electrospray (ES) ionization techniques. ATR-FTIR spectra were recorded using an Agilent Cary 630 spectrometer with a diamond ATR module, averaging 128 scans for each spectrum. A Remet TC10 universal testing machine was used to perform all the tensile and flexural tests. The instrument was equipped with a 1 KN cell, with a crosshead speed of 1 mm min^{-1} for tensile test, according to the ISO 37 Type 2. Hardness was evaluated using an analogic Shore D durometer (Remet).

Thermogravimetric analysis (TGA) was performed using a Discovery TGA (TA Instruments, USA) under a N_2 atmosphere with a gas flow of 100 mL min^{-1} and a heating rate of 10 °C min^{-1} from 30 °C to 600 °C.

Differential scanning calorimetry (DSC) measurements were carried out using a Q2000 DSC (TA Instruments, USA) under a nitrogen atmosphere with a flow rate of 50 mL min^{-1}. Samples were sealed in aluminium pans and subjected to a heating–cooling–heating cycle: first heating from room temperature to 180 °C, cooling to −80 °C, and a second heating up to 180 °C, all at a rate of 10 °C min^{-1}. The instrument was calibrated according to the manufacturer's standard procedures.

Green metrics

The biobased cabon content of each formulation was calculated according to eqn (1), as previously reported.[24] For a formulation including n components i, each with its own weight fraction w_i:

$$\mathrm{BCC}_{\%} = \frac{\text{Total biobased carbon mass}}{\text{Total carbon mass}} = \frac{\sum_{i=1}^{n} w_i \mathrm{C}_{\%,i} \frac{n_{\mathrm{BC},i}}{n_{\mathrm{C},i}}}{\sum_{i=1}^{n} w_i \mathrm{C}_{\%,i}} \quad (1)$$

where $C_{\%,i}$ is the total carbon content of each component i, $n_{BC,i}$ is the number of biobased carbon atoms in its molecular structure and $n_{C,i}$ is the total number of carbon atoms in the molecules of component i.

The Sustainable Formulation Score (SFS) was calculated for each formulation according to its definition (eqn (2)).[5]

For a formulation including n components i, each with its own weight fraction w_i:

$$\mathrm{SFS} = 100 \cdot F_{\mathrm{EoL}} \cdot \sum_{i=1}^{n} \left(w_i \cdot \mathrm{BCC}_i \cdot F_{\mathrm{syn},i} \right) \quad (2)$$

where F_{EoL} is defined as the end-of-life factor, and $\sum_{i=1}^{n} (w_i \cdot \mathrm{BCC}_i \cdot F_{\mathrm{syn},i})$ is the weighted sum of the synthetic factors F_{syn} of each component multiplied by the corresponding biobased carbon content, calculated for each component according to eqn (1).

Results and discussion

The synthesis of the new amino acid (AA)–derived itaconamide monomers proceeded through three main steps (Fig. 1): (i) esterification of the amino acid, (ii) nucleophilic ring-opening of itaconic anhydride to form the corresponding itaconamide intermediate (IA), and (iii) final esterification of the free carboxyl group. In this work, selected AAs are alanine (Ala), valine (Val), isoleucine (Ile), and phenylalanine (Phe).

Synthesis of MEIA derivatives

Methanol/sulfuric acid Fischer esterification afforded the corresponding methyl esters in quantitative yield, with reaction times adjusted for each amino acid. The ring-opening of itaconic anhydride was then carried out following conditions inspired by Slusher *et al.*, with specific adjustments depending on the nature of each amino ester.[25] The optimized conditions allowed high conversions and generally quantitative yields for all intermediates. Following anhydride opening, a second esterification step afforded the final MEIA monomers (Fig. 2). Ala-MEIA and Phe-MEIA were isolated as solids, while Oct-MEIA, Ile-MEIA, and Val-MEIA remained liquid, likely due to different combinations of polarity, side-chain packing, and intermolecular interactions (including π-stacking in the case of phenylalanine). Despite these differences, all monomers were readily soluble in the resin mixtures used for formulation. A key advantage of this synthetic route is its high atom economy and avoidance of hazardous activating reagents such as itaconoyl chlorides or epoxides, which are frequently used in literature for similar transformations.[19,20] In addition, under the selected conditions the formation of Aza-Michael by-products, commonly observed for amine reactions with itaconic derivatives, was not detected, confirming that the ring-opening pathway was strongly favoured.[26]

All MEIA derivatives were characterized by NMR, ATR-FTIR, and ESI-MS, confirming successful progression through each step.

As expected, the ^{1}H-NMR spectra (Fig. S1–S20) show the complete disappearance of the anhydride resonances and the concomitant appearance of characteristic amide N–H and vinyl signals, confirming the successful nucleophilic ring opening of itaconic anhydride and formation of the corresponding itaconamide derivatives. The reaction proceeds regioselectively through preferential attack at the thermodynamically favored carbonyl, leading predominantly to the α,β-ring-opened product. This thermodynamic regiocontrol is consistent with the formation of a resonance-stabilized unsaturated carboxylate intermediate and is in agreement with established literature precedents.[27] As a consequence of the newly formed stereogenic

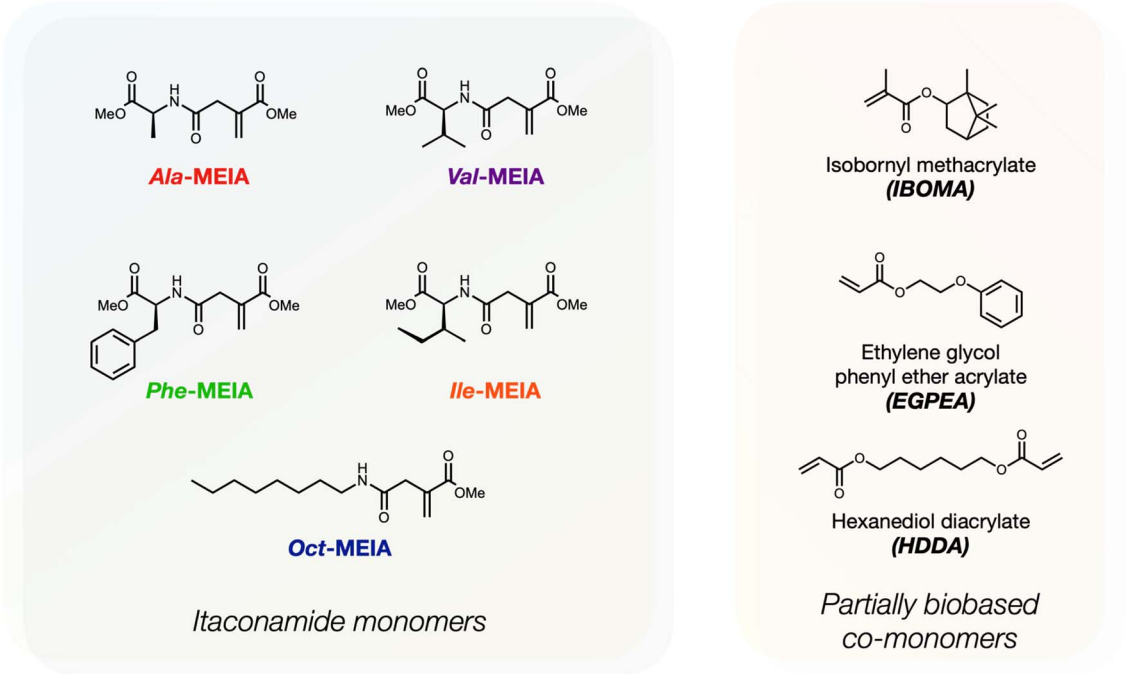

Fig. 2 Chemical structure of the synthesized amino acid–based photocurable monomers.

environment, the methylene protons adjacent to the amide group become diastereotopic in Phe-, Ile-, and Val-MEIA derivatives, while they remain magnetically equivalent and appear as singlets in the alanine- and octylamine-based analogues, in line with the expected molecular symmetry. Notably, the minor vinyl resonances previously attributed to the α,β-coproduct in the IA intermediates were no longer detected after final purification of the MEIAs, likely due to signal shifting associated with the altered electronic environment upon ester formation.

ATR-FTIR spectra (Fig. S21) further support the successful formation of the amide and ester groups. The N–H stretching band at approximately 3325 cm^{-1} and the Amide II band near 1540 cm^{-1} are present for all compounds. The anhydride C=O signals (1830–1764 cm^{-1}) disappear after ring opening, replaced by the characteristic ester and amide carbonyl stretching bands at lower wavenumbers. Mass spectrometry analysis confirmed the expected molecular weights for all MEIA derivatives. Together, these results verify that the synthetic sequence reliably yields the desired sustainable monomers.

Formulation of photocurable resins and VP 3D printing

Once the desired monomers were obtained, three resin formulations were prepared for each amino acid–derived MEIA by progressively increasing its molar contribution to the total amount of photocurable double bonds (10, 25, and 40 mol%, Table S2). Each formulation was produced by incorporating the MEIA monomer into a reference resin composed of isobornyl methacrylate (IBOMA), ethylene glycol phenyl ether acrylate (EGPEA), and hexanediol diacrylate (HDDA). Starting from a baseline system composed of 45 wt% IBOMA and EGPEA and 10 wt% HDDA, the MEIA content was increased while maintaining two parameters strictly constant across all formulations:

(i) the 1 : 1 weight ratio between the monofunctional components IBOMA and EGPEA, and

(ii) the molar contribution of the difunctional crosslinker HDDA, fixed at 16.8 mol% of the total acrylate double bonds. These constraints were intentionally imposed to isolate the effect of the MEIA molecular structure on the final mechanical properties, avoiding artefacts due to variations in mono-/diacrylate ratios or changes in crosslink density.

Resin preparation was carried out by mechanical mixing. Despite the typically limited solubility of amide-containing molecules in hydrophobic media, all synthesized monomers dissolved readily in the resin blend under simple mechanical agitation. In particular, Oct-MEIA, Ile-MEIA, and Val-MEIA showed excellent solubility, as these compounds were obtained as non-crystalline amorphous materials after synthesis. This behavior is attributed to their molecular structure, including increased conformational flexibility, steric hindrance, and, in the case of branched amino acid derivatives, reduced packing efficiency and the presence of multiple stereogenic environments, which hinder crystallization during solvent removal rather than indicating an intrinsically liquid phase. After achieving a homogeneous mixture, ethyl (2,4,6-trimethyl benzoyl) phenyl phosphinate (Et-APO, 2.0 wt%) and 2,6-di-*tert*-butyl-4-methylphenol (BHT, 0.5 wt%) were added as the photoinitiator and stabilizer, respectively. The resulting formulations were processed by vat photopolymerization. Exposure times were optimized for each MEIA content and monomer type, resulting in values between 50 and 120 s per layer. These irradiation times are noticeably longer than those typically used for commercial acrylate or methacrylate systems (around 20 s per layer), a behaviour that is fully consistent with the intrinsically lower photoreactivity of amide-containing

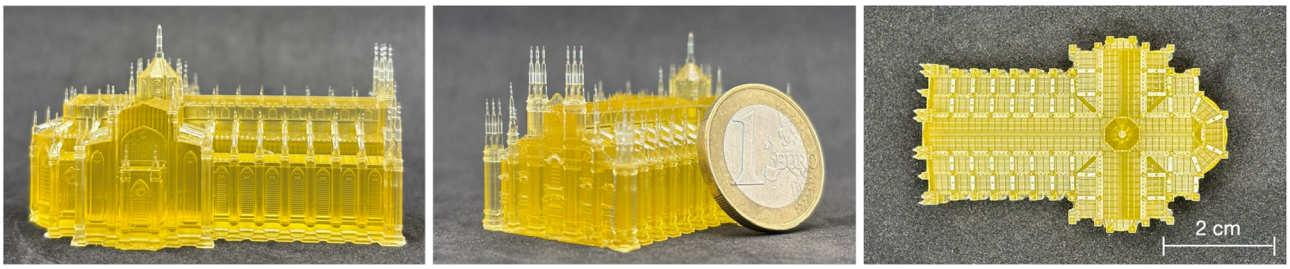

Fig. 3 3D printing performances of MEIA-based resins. High-resolution 3D-printed reproduction of Milan's Dome printed using 40 mol% of Ile-MEIA. Object size is 39 × 60 × 33 mm, spiers are as thin as 0.5 mm.

monomers and itaconic structures, which require prolonged exposure to achieve complete polymer conversion.[28] Importantly, the exposure times required for these formulations remain within the range previously reported for itaconic acid–based photocurable resins, confirming that the incorporation of MEIA monomers does not introduce additional limitations in terms of printability. After printing, all specimens underwent a 2 h post-curing step at 60 °C under UV irradiation to ensure full network formation.

To evaluate the printing resolution achievable with the MEIA-based formulations, a complex architectural model (Milan's Dome, Fig. 3) was fabricated using 40 mol% of Ile-MEIA. The printed structure reproduced spires with diameters below 0.5 mm, confirming the suitability of these monomers for high-precision features. A second benchmark object was also successfully produced (Fig. S24), incorporating challenging geometrical elements such as a vertical through-hole, bridges up to 16 mm in length, sharp spikes, overhangs with inclinations up to 70°, and walls progressively thinning down to 0.1 mm. The successful reproduction of these fine and demanding details demonstrates that, under the adopted photopolymerization conditions, the amino acid–derived resins retain excellent print fidelity and support the high-resolution performance typically associated with VP processes.

Mechanical properties of 3D printed materials

Tensile tests performed on ISO 37 Type 2 specimens (Table S8 and Fig. S22) reveal that the incorporation of MEIA monomers consistently softens the photocrosslinked network relative to the blank formulation, while the extent and nature of this effect depend strongly on the structure of the amino acid residue. Across all monomers, the elastic modulus decreases upon MEIA addition, accompanied by variable reductions in tensile strength and, except for the phenylalanine derivative, significant increases in elongation at break. These observations indicate that the introduction of itaconamide units disrupts the packing and regularity of the acrylate–methacrylate network, lowering stiffness and promoting segmental mobility.

Clear structure–property relationships emerge when comparing the mechanical responses of the different MEIAs. Oct-MEIA, containing a long linear C8 chain, acts as an efficient internal plasticizing segment and provides the most ductile materials in the series, with the elongation of the 40 mol% formulation increasing by +385% relative to the blank, accompanied by substantial decreases in modulus and tensile strength. Ile-MEIA, bearing a branched aliphatic chain, produces a similarly pronounced softening effect, with elongation improving by +300% at 40 mol% loading, consistent with reduced packing efficiency and enhanced chain mobility, while gradually decreasing modulus and tensile strength. Val-MEIA, with a shorter branched side group, yields intermediate behaviour: elongation increases by +186% at high loading, while tensile strength and modulus remain comparatively higher than for Oct- or Ile-based systems, reflecting the weaker steric disruption imparted by its smaller substituent. Despite the relatively small molecular difference between Val-MEIA and Ile-MEIA, a marked increase in elongation at break is observed upon incorporation of the slightly bulkier comonomer. Similar sensitivity to subtle variations in (meth)acrylate side-chain structure has been reported in the literature, where minor structural changes between monofunctional comonomers such as isodecyl acrylate and 2-ethylhexyl methacrylate were shown to induce pronounced differences in thermal behavior and elastic modulus.[29]

In contrast, Ala-MEIA exhibits an unexpectedly strong reduction in modulus (−68%) and tensile strength (−49%) at 40 mol% despite its minimal steric bulk. This behaviour is likely related to its reduced solubility in the resin mixture and the formation of local inhomogeneities in the printed network, which increase defect density and compromise mechanical performance. A distinct trend is observed for Phe-MEIA: at low incorporation levels (10 mol%), the aromatic residue reinforces the network slightly, increasing tensile strength to 40 MPa (+20% compared to blank resin). At higher contents, however, both strength and ductility decline markedly, with elongation dropping below that of the blank. This non-monotonic response is consistent with π–π interactions between phenyl groups, which may promote micro-aggregation or partial gelling at elevated concentrations, impairing resin homogeneity and restricting extensibility.[30,31]

Finally, hardness remains largely unaffected across the series, with several formulations matching or slightly exceeding the reference material. This confirms that surface rigidity is preserved upon incorporation of these monomers (Table S8).

Overall, the tensile results highlight a consistent and largely advantageous effect of AA-MEIA incorporation on the mechanical performance of the printed materials relative to the blank

resin (Fig. 4). Increasing MEIA content systematically amplifies the trends described above and is accompanied by a larger dispersion of the measured values, reflecting the heightened sensitivity of the photocrosslinked network to monomer distribution, local polymerization kinetics, and compositional heterogeneities at higher loadings. While the introduction of itaconamide units invariably reduces network stiffness, this effect is coupled with pronounced gains in deformability and, in several cases, only moderate reductions-or even local improvements-in tensile strength, resulting in mechanically more compliant yet still robust materials. In particular:

• the elastic modulus decreases consistently across all MEIA derivatives, confirming effective network softening regardless of side-chain chemistry and indicating progressive disruption of acrylate–methacrylate packing as MEIA content increases;

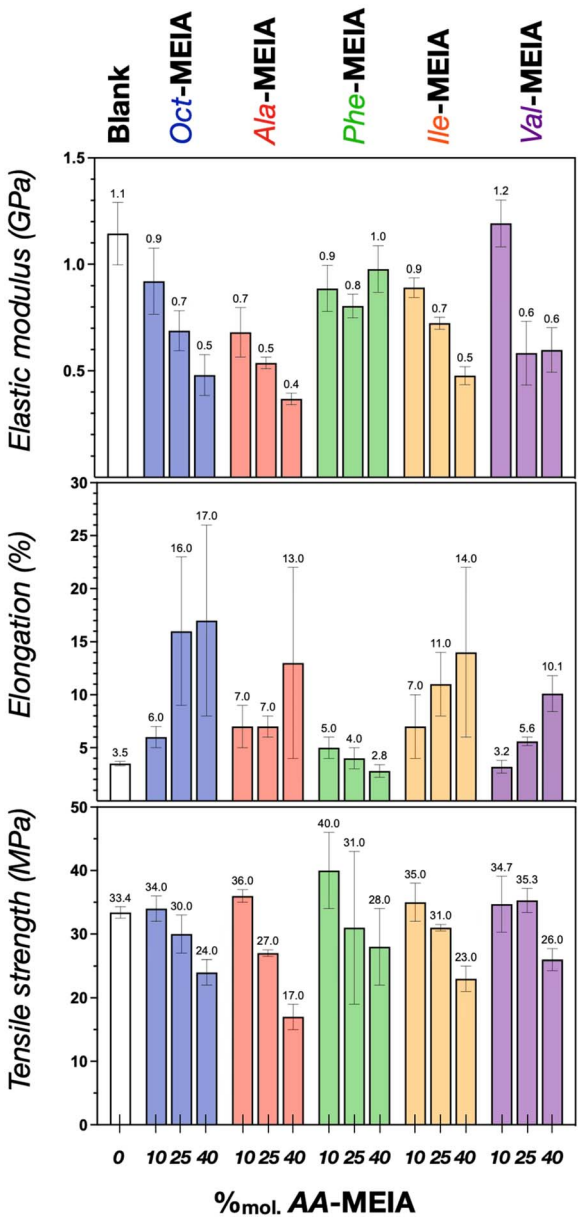

Fig. 4 Tensile properties of MEIA-based resins. Data are represented as mean ± SD of a minimum of 5 independent replicates.

• the elongation at break exhibits the most pronounced and systematic enhancement, especially for aliphatic MEIAs, with long or branched side chains promoting substantial flexibility gains, while smaller substituents induce softening but may introduce local heterogeneities when solubility becomes limiting.

• the tensile strength averages consistent or slightly higher values to the blank ones for 10% formulations, despite the general decrease observed with increasing MEIA loading; still, it remains comparatively well preserved for intermediate aliphatic residues and can even increase at low aromatic contents, whereas higher concentrations of Phe-MEIA lead to embrittlement, consistent with the onset of π–π interactions and reduced network homogeneity.

Taken together, these results demonstrate that the mechanical response of MEIA-based materials can be finely tuned through rational modulation of the amino acid side-chain structure and its concentration. Long or branched aliphatic substituents primarily enhance flexibility, small residues soften the network with a higher sensitivity to dispersion effects, and aromatic groups introduce secondary interactions that can either reinforce or embrittle the network depending on loading. This structure–property tunability provides a versatile and effective strategy for tailoring the performance of bio-based photocurable resins for vat photopolymerization.

Finally, hardness remains largely unaffected across the series, with several formulations—particularly Phe-MEIA40 and the aliphatic derivatives at 10–25 mol%—matching or slightly exceeding the reference material. This confirms that surface rigidity is preserved upon incorporation of these monomers (Table S8).

Thermal properties of 3D printed materials

Thermogravimetric analysis (TGA) was performed on the 3D-printed materials to evaluate the effect of AA-MEIA incorporation on thermal stability (Fig. 5a, S23 and Table S9). The blank resin and Oct-MEIA 40 display two main degradation steps, with DTG maxima at approximately 300–310 °C and 410–415 °C, attributable to the decomposition of the acrylate matrix followed by the breakdown of more stable crosslinked fragments. In contrast, all amino acid–derived MEIA formulations exhibit an additional degradation event at lower temperature, which becomes clearly resolved for Phe-MEIA and Ile-MEIA (DTG maxima at ∼250 °C and ∼238 °C, respectively) and appears as a shoulder for Ala-MEIA and Val-MEIA. This low-temperature process is attributed to the initial decomposition of the amino acid–derived itaconamide segments, consistent with reported degradation pathways of amino acids involving decarboxylation and deamination in the 200–300 °C range.

The clearer separation observed for Phe- and Ile-MEIA is likely related to the increased steric bulk and hydrophobicity of their side chains, which promote a more kinetically distinct degradation step, whereas smaller residues lead to overlapping processes with the onset of matrix decomposition. A further distinguishing feature is the residue at 600 °C. While the blank resin leaves only 1.2 wt% residue and Oct-MEIA 40 reaches 4.0 wt%, all amino acid–containing formulations yield

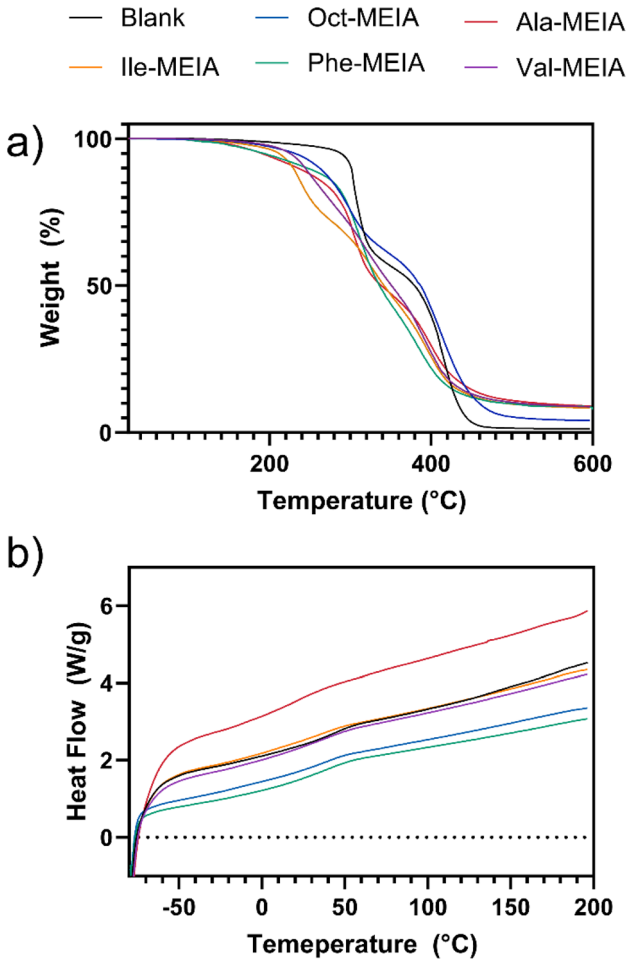

Fig. 5 TGA (a) and DSC (b) curves of photocured resins containing 40 mol% of the different synthesized itaconamides.

significantly higher char contents (8–9 wt%). This trend indicates that nitrogen-containing itaconamide units enhance condensed-phase stabilization during pyrolysis, in agreement with literature on amide-bearing polymer networks. The markedly lower residue of Oct-MEIA highlights the decisive role of the substituent chemistry, with amino acid–derived structures being more effective than simple aliphatic chains in promoting char formation.

Differential scanning calorimetry (DSC) thermograms of all formulations are essentially identical (Fig. 5b), showing only a weak and broad glass-transition-like step near room temperature. This behaviour is typical of densely crosslinked acrylate networks and indicates that MEIA incorporation, irrespective of amino acid side-chain structure, does not significantly affect the pre-decomposition thermal transitions or segmental mobility of the matrix.

Sustainability of MEIA-based formulation

Assessing the sustainability of photocurable formulations cannot be limited to reporting the bio-based carbon content ($BCC_{\%}$), which is still the most frequently used indicator in the literature but provides only a partial view of a material's overall environmental performance. Recent analyses have clearly demonstrated that the renewable origin of a feedstock does not necessarily correlate with lower environmental impact, as other factors – such as the degree of functionalization, the use of catalysts or additives, the energy intensity of synthetic steps, and the end-of-life compatibility of the resulting networks – play equally significant roles. Standard metrics like $BCC_{\%}$ fail to capture these aspects and can be misleading if used in isolation, motivating the development of more holistic sustainability indicators.[32] To obtain a more comprehensive and comparable assessment, in this work we quantify the sustainability of our formulations using the Sustainable Formulation Score (SFS), following the criteria and weighting scheme established in recent literature.[5] The SFS enables integration of multiple dimensions of sustainability beyond bio-based content, capturing aspects of molecular design, synthetic efficiency, and expected end-of-life behavior. A summary of the calculated SFS values for all formulations is provided in Table 1. The values assigned for each synthetic subfactor for the calculation of the SFSs are provided in Table S10. The SFS analysis highlights a substantial differentiation in sustainability performance across the series, with several formulations achieving values that place them among the most sustainable photocurable systems reported to date. While the incorporation of MEIA monomers results in only moderate increases in bio-based carbon content, the corresponding rise in SFS is much more pronounced. In particular, formulations enriched in Ala-MEIA, Phe-MEIA, Ile-MEIA, and Val-MEIA at 40 wt% consistently reach SFS values between 46.7 and 51.8. These values exceed those reported for the vast majority of bio-based or partially bio-derived resins surveyed in recent literature, where SFS scores above 40 remain relatively uncommon and only a few advanced systems surpass the threshold of 50. This positioning is especially evident for Phe-MEIA40 (SFS = 51.8), which stands at the uppermost end of the sustainability spectrum among currently published photocurable formulations, with Ala-MEIA40, Ile-MEIA40, and Val-MEIA40 following closely. Even at

Table 1 Sustainability metrics for the reported formulations. $BCC_{\%}$ = biobased carbon content and SFS = sustainable formulation score

Resin ID	$BCC_{\%}$	SFS	
Blank	45.0%	18.1	●
Oct-MEIA 10	44.6%	20.3	●
Oct-MEIA 25	44.0%	23.4	●
Oct-MEIA 40	43.5%	26.3	●
Ala-MEIA 10	49.4%	25.3	●
Ala-MEIA 25	56.5%	36.1	●
Ala-MEIA 40	64.2%	46.7	●
Phe-MEIA 10	51.8%	27.6	●
Phe-MEIA 25	61.5%	40.4	●
Phe-MEIA 40	70.4%	51.8	●
Ile-MEIA 10	50.3%	26.6	●
Ile-MEIA 25	58.3%	38.6	●
Ile-MEIA 40	66.5%	49.7	●
Val-MEIA 10	50.5%	26.6	●
Val-MEIA 25	58.8%	38.5	●
Val-MEIA 40	67.2%	49.7	●

intermediate MEIA loadings (25 wt%), several systems attain SFS values in the 36–40 range, already aligning with or exceeding those of the most competitive bio-based resins described in the literature benchmark. Overall, these results demonstrate that MEIA-based formulations do not simply match existing sustainable materials but outperform them in many cases, positioning this molecular platform as one of the most promising routes toward genuinely high-sustainability photocurable resins.

This comparison becomes particularly meaningful when contextualized within the broader literature on so-claimed bio-based or bio-derived photocurable resins. In many reported systems, sustainability claims are largely driven by the renewable origin of the monomers, while formulation complexity, often involving highly functionalized acrylates, petroleum-derived reactive diluents, photoinitiators, and stabilizers, substantially limits the resulting sustainability performance. Consequently, despite bio-based carbon contents that are sometimes comparable to those reported here, SFS values frequently remain below 35–40, highlighting the limited impact of renewable feedstock substitution alone when not accompanied by molecular- and formulation-level simplification.[33–35] In particular, a large fraction of bio-based photocurable formulations relies on multifunctional monomers derived from plant oils, lignin fragments, terpenes, or sugars, which require extensive chemical modification to introduce photoreactive groups.[36,37] These additional functionalization steps increase synthetic complexity, energy demand, and auxiliary reagent use, factors that are explicitly captured by the SFS methodology but remain invisible when sustainability is assessed solely through $BCC_{\%}$. As a result, even formulations marketed as "highly bio-based" frequently achieve only moderate SFS scores, underscoring a structural limitation of many current bio-monomer strategies.[38,39]

Against this backdrop, the performance of MEIA-based formulations is particularly noteworthy. The pronounced increase in SFS observed upon MEIA incorporation reflects not only the renewable origin of the amino acid feedstocks, but also the favorable balance between molecular simplicity, limited functionalization, and effective performance at relatively high loadings. This combination allows MEIA-rich formulations to surpass the sustainability benchmarks of most reported bio-based systems, rather than merely aligning with them. Consequently, these results position amino acid–derived itaconamides as a distinct and highly competitive class of building blocks, capable of delivering genuinely high-sustainability photocurable resins rather than incremental improvements over existing bio-based formulations.

Conclusions

This work presents a sustainable and modular strategy for the development of photocurable resins for vat photopolymerization based on amino acid–derived itaconamide monomers. By exploiting the direct ring-opening of itaconic anhydride with amino acid derivatives, a family of biobased monomers was synthesized through a simple, high-atom-economy route that avoids hazardous activating agents and multistep functionalization, in full alignment with green chemistry principles. The incorporation of MEIA monomers at up to 40 mol% enables effective and predictable tuning of mechanical properties while preserving excellent printability and resolution. Aliphatic amino acid derivatives act as efficient internal plasticizers, producing large increases in elongation at break (up to +385% relative to the blank) while maintaining adequate tensile strength and surface hardness. In contrast, the phenylalanine-based monomer introduces secondary aromatic interactions that allow selective network reinforcement at low loadings, demonstrating how side-chain chemistry can be used to modulate network response. Importantly, all formulations retain thermal stability and dimensional accuracy fully compatible with vat photopolymerization requirements.

Beyond material performance, the sustainability of the developed formulations was quantitatively assessed using the Sustainable Formulation Score (SFS), providing a holistic evaluation that extends beyond conventional biobased carbon content metrics. Several MEIA-rich formulations achieve SFS values between 46.7 and 51.8, placing them among the most sustainable non-recyclable photocurable resins reported to date and clearly outperforming the majority of state-of-the-art bio-based VP systems.

Overall, this study demonstrates that meaningful advances in sustainable 3D-printing vat photopolymerization require the integration of renewable feedstocks with simplified synthetic routes and formulation-level efficiency. Amino acid–derived itaconamides (MEIA) emerge as a versatile and competitive molecular platform, capable of delivering high-resolution, mechanically tunable, and quantitatively more sustainable photocurable resins, and represent a promising pathway toward next-generation additive manufacturing materials.

Author contributions

Conceptualization: MCF. Data curation: FC, RC, MM, EL. Funding acquisition: MCF, SIM. Investigation: RC, FC, LS. Methodology: RC, FC, EL, MM, LS. Supervision: writing – original draft: MCF. Writing – review and editing: MM, RC, FC, SIM.

Conflicts of interest

There are no conflicts to declare.

Data availability

All data supporting this article as all the chemical, thermomechanical characterization and the SFS calculation are provided within the manuscript and the supplementary information (SI). Supplementary information is available. See DOI: https://doi.org/10.1039/d6su00014b.

Acknowledgements

This research was funded by Project Ecosister—Ecosystem for Sustainable Transition in Emilia-Romagna, Project funded

under the National Recovery and Resilience Plan (NRRP), Mission 04 Component 2 Investment 1.5 – NextGenerationEU, Call for tender n. 3277 dated 30/12/2021, Award Number: 0001052 dated 23/06/2022, within Spoke 1 activities—Materials for sustainability and ecological transition—(CUP J33C22001240001). MM and SI acknowledge funding from the Spanish Ministry of Science, Innovation, and Universities MICIU/AEI/10.13039/501100011033 (Project PID2023-151632OB-C22) and from FEDER, EU.

Notes and references

1 ASTM Wohlers Report, 2025, https://www.astm.org/news/press-releases/wohlers-report-2025.
2 M. Shah, A. Ullah, K. Azher, A. U. Rehman, W. Juan, N. Aktürk, C. S. Tüfekci and M. U. Salamci, *RSC Adv.*, 2023, **13**, 1456–1496.
3 S. Subedi, S. Liu, W. Wang, S. M. A. Naser Shovon, X. Chen and H. O. T. Ware, *npj Adv. Manuf.*, 2024, **1**, 9.
4 V. S. D. Voet, J. Guit and K. Loos, *Macromol. Rapid Commun.*, 2021, **42**, 2000475.
5 M. Maturi, E. Locatelli, A. S. de Leon, M. C. Franchini and S. I. Molina, *Green Chem.*, 2025, **27**, 8710–8754.
6 R. Saraswat, S. Shagun, A. Dhir, A. S. S. Balan, S. Powar and M. Doddamani, *RSC Sustainability*, 2024, **2**, 1708–1737.
7 L. Pezzana, R. Wolff, J. Stampfl, R. Liska and M. Sangermano, *Addit. Manuf.*, 2024, **79**, 103929.
8 S. Grauzeliene, M. Kastanauskas, V. Talacka and J. Ostrauskaite, *ACS Appl. Polym. Mater.*, 2022, **4**, 6103–6110.
9 I. Cazin, M. Ocepek, J. Kecelj, A. S. Stražar and S. Schlögl, *Materials*, 2024, **17**, 1890.
10 A. Navaruckiene, E. Skliutas, S. Kasetaite, S. Rekštytė, V. Raudoniene, D. Bridziuviene, M. Malinauskas and J. Ostrauskaite, *Polymers*, 2020, **12**, 397.
11 T. Wu, S. Sugiarto, R. Yang, T. Sathasivam, U. A. Weerasinghe, P. L. Chee, O. Yap, G. Nyström and D. Kai, *Mater. Horiz.*, 2025, **12**, 2789–2819.
12 R. T. Alarcon, M. Bergoglio, É. T. G. Cavalheiro and M. Sangermano, *Polymers*, 2025, **17**, 587.
13 T. Robert and S. Friebel, *Green Chem.*, 2016, **18**, 2922–2934.
14 F. Kong, X. Ma, X. Xu, M. Cui, H. Zhao, J. Zhu and J. Chen, *Mater. Today Chem.*, 2024, **35**, 101881.
15 M. Maturi, C. Spanu, E. Locatelli, L. Sambri and M. Comes Franchini, *Addit. Manuf.*, 2024, **92**, 104360.
16 R. Carmenini, A. Sanz De León, T. Benelli, L. Giorgini, M. Comes Franchini, S. I. Molina and M. Maturi, *Green Chem.*, 2025, **27**, 12830–12843.
17 V. S. D. Voet, J. Guit and K. Loos, *Macromol. Rapid Commun.*, 2021, **42**, 2000475.
18 T. Werpy and G. Petersen, *Top Value Added Chemicals from Biomass: Volume I – Results of Screening for Potential Candidates from Sugars and Synthesis Gas*, 2004.
19 J.-T. Miao, S. Peng, M. Ge, Y. Li, J. Zhong, Z. Weng, L. Wu and L. Zheng, *ACS Sustainable Chem. Eng.*, 2020, **8**, 9415–9424.
20 C. Spanu, E. Locatelli, L. Sambri, M. C. Franchini and M. Maturi, *ACS Appl. Polym. Mater.*, 2024, **6**, 2417–2424.
21 R. Carmenini, M. D. Donne, E. Locatelli, L. Sambri, L. Giorgini, L. Mazzocchetti and M. C. Franchini, *ACS Sustain. Chem. Eng.*, 2025, **13**, 12421–12429.
22 R. Carmenini, C. Spanu, E. Locatelli, L. Sambri, M. C. Franchini and M. Maturi, *Progr. Addit. Manuf.*, 2024, **9**, 2499–2510.
23 R. A. Sheldon, *Green Chem.*, 2007, **9**, 1273.
24 D20 Committee, *Test Methods for Determining the Biobased Content of Solid, Liquid, and Gaseous Samples Using Radiocarbon Analysis*, ASTM D6866-20.
25 B. Slusher, M. Islam, R. Rais, L. Garza, B. Bell, P. Majer, L. Tenora, I. Snajdr and M. Krecmerova, *World Intellectual Property Organization Pat.*, WO2021087082A1, 2021.
26 P. L. Paytash, E. Sparrow and J. C. Gathe, *J. Am. Chem. Soc.*, 1950, **72**, 1415–1416.
27 M. Maturi, C. Spanu, E. Locatelli, L. Sambri and M. Comes Franchini, *Addit. Manuf.*, 2024, **92**, 104360.
28 L. Sollka and K. Lienkamp, *Macromol. Rapid Commun.*, 2021, **42**, 2000546.
29 D. L. Safranski and K. Gall, *Polymer*, 2008, **49**, 4446–4455.
30 C. A. Hunter and J. K. M. Sanders, *J. Am. Chem. Soc.*, 1990, **112**, 5525–5534.
31 D. P. Královič, K. Cifraničová, H. Švajdlenková, D. Tóthová, O. Šauša, P. Kalinay, T. Kavetskyy, J. Ostrauskaite, O. Smutok, M. Gonchar, V. Soloviev and A. Kiv, *J. Polym. Environ.*, 2024, **32**, 2336–2349.
32 J.-G. Rosenboom, R. Langer and G. Traverso, *Nat. Rev. Mater.*, 2022, **7**, 117–137.
33 B. Wu, A. Sufi, R. Ghosh Biswas, A. Hisatsune, V. Moxley-Paquette, P. Ning, R. Soong, A. P. Dicks and A. J. Simpson, *ACS Sustainable Chem. Eng.*, 2020, **8**, 1171–1177.
34 C. Vazquez-Martel, L. Becker, W. V. Liebig, P. Elsner and E. Blasco, *ACS Sustainable Chem. Eng.*, 2021, **9**, 16840–16848.
35 C. Mendes-Felipe, I. Isusi, O. Gómez-Jiménez-Aberasturi, S. Prieto-Fernandez, L. Ruiz-Rubio, M. Sangermano, J. L. Vilas-Vilela, C. Mendes-Felipe, I. Isusi, O. Gómez-Jiménez-Aberasturi, S. Prieto-Fernandez, L. Ruiz-Rubio, M. Sangermano and J. L. Vilas-Vilela, *Polymers*, 2023, **15**, 3136.
36 P. Zhang and J. Zhang, *Green Chem.*, 2013, **15**, 641–645.
37 P. Zhang, J. Xin and J. Zhang, *ACS Sustainable Chem. Eng.*, 2014, **2**, 181–187.
38 L. Papadopoulos, L. Pezzana, N. M. Malitowski, M. Sangermano, D. N. Bikiaris and T. Robert, *ACS Omega*, 2023, **8**, 31009–31020.
39 L. Papadopoulos, N. M. Malitowski, D. Bikiaris and T. Robert, *Eur. Polym. J.*, 2023, **186**, 111872.